SPECTROPOLARIMETRIC PROPERTIES OF THE LUNAR SWIRL REINER GAMMA AND WESTERN OCEANUS PROCELLARUM. C. Wöhler[1], M. Bhatt[2], M. Arnaut[1], S. Ganesh[2], K. Aravind[2], A. Bhardwaj[2]. [1]Image Analysis Group, TU Dortmund University, 44227 Dortmund, Germany, christian.woehler@tu-dortmund.de, [2]Physical Research Laboratory, Ahmedabad, 380009, India, megha@prl.res.in.

Introduction: The sunlight reflected by the lunar surface is partially linearly polarized to a variable extent in dependence on the phase angle. Polarization provides information about the grain size and microscopic roughness of the regolith [1, 2]. Wavelength-dependent polarimetric analysis provides insight into the internal structure of the regolith grains [3]. In this work, we present new telescopic multispectral imaging polarimetric data of western Oceanus Procellarum with special focus on the swirl structure Reiner Gamma.

Data and Methods: Spectropolarimetric image dataset 1 was acquired on February 22nd, 2022, at a phase angle of 64.4° with the 1 m reflector of the Mount Abu observatory in Rajasthan, northern India, equipped with the EMPOL imaging polarimeter [4]. The image scale is 0.6 km per pixel, the covered spectral bands are BC, GC and RC (Table 1). For each of the 48 orientation angles of the EMPOL polarizer, 7-11 individual frames were coregistered and stacked.

Dataset 2 was acquired on December 16th, 2022, at a phase angle of 87.5° with a 200 mm Newton reflector located near Dortmund, Germany. The primary focal length of 1.2 m was extended to 3.0 m with a Barlow lens. As a polarimetric imaging sensor, we used a monochrome The Imaging Source DZK 33GX250 industrial polarization camera whose individual sensor pixels are equipped with polarization filters rotated by 0°, 45°, 90° and 135° [5]. The image scale is 0.9 km per pixel, the covered spectral bands are U, B, G, R and I (Table 1). In each band a set of 3500 individual frames was taken. After reading out the individual sub-frames corresponding to the four polarization directions, the sharpest 10% of the sub-frames were stacked with the software Autostakkert3 [6].

For both datasets, the stacked images were used to infer the linear polarization state as given by the pixel intensity F, the fraction P of linearly polarized light, and the orientation angle W of the polarization plane. Typical P spectra are shown in Fig. 1. A Principal Component Analysis (PCA) was applied to the band-wise P data, and the scores on the first three principal components PC1, PC2 and PC3 were visualized as color composite and grayscale maps (Figs. 2 and 3). Furthermore, a Clementine-style [7] logarithmic intensity ratio composite was constructed for the qualitative illustration of spectral units (Fig. 2).

Results and Discussion: In Fig. 2, the units apparent in the PCA composite largely correspond to those of the intensity ratio composite, which is due to the general anti-correlation between P and albedo known as the Umov law [1]. Deviations from this trend are visible in the PCA composite, e.g., at Reiner Gamma, the southern outer rim of Aristarchus and some rays of Kepler. Such deviations from the general trend may be interpreted as variations in grain size [1, 2, 3]. Additionally, our local PCA analysis of the Reiner Gamma area (Fig. 3) shows distinct differences in the PC3 score for the main oval on the one hand and the north-eastern tail and southwestern patches on the other hand. This behavior indicates variations in the structural properties of the swirl's regolith on kilometer scales, suggesting that beyond a mere magnetic shielding of the surface from the solar wind [8], an external force such as the interaction between the regolith and the gaseous hull of a passing comet (e.g., [9]) contributed to the formation of the swirl.

BC	GC	RC	U	B	G	R	I
445	526	713	369	470	520	632	890

Table 1: Center wavelengths (in nm) of the spectral bandpass filters used in datasets 1 [10] and 2 [11].

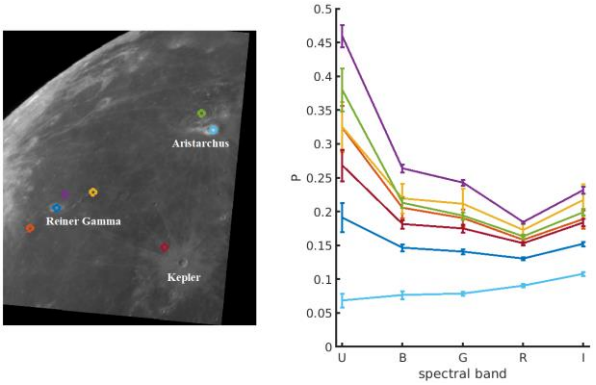

Figure 1: Intensity (F) image of western Oceanus Procellarum (dataset 2) with selected locations marked by colored circles, corresponding P spectra (mean and standard deviation over areas of 5 × 5 pixels, respectively).

References: [1] Shkuratov, Y. and Opanasenko, N. (1992) Icarus 99(2), 468-484. [2] Dollfus, A. (1998) Icarus 136(1), 69-103. [3] Shkuratov, Y. et al. (2007) Icarus 187(2), 406-416. [4] Ganesh, S. et al. (2020) SPIE Vol. 11447, 2032-2038. [5] The Imaging Source (2019) https://www.theimagingsource.com/products/industrial-cameras/gige-polarsens/dzk33gx250/ [6] Kraaikamp, E. (2023) https://www.autostakkert.com [7] Pieters, C. M. et al. (1994) Science 266(5192), 1844-1848. [8] Glotch, T. et al. (2015) Nature Comm. 6, 6189. [9] Hess, M. et al. (2020) A&A 639, A12. [10] Farnham, T. L. et al. (2000) Icarus 147(1), 180-204. [11] https://www.baader-planetarium.de

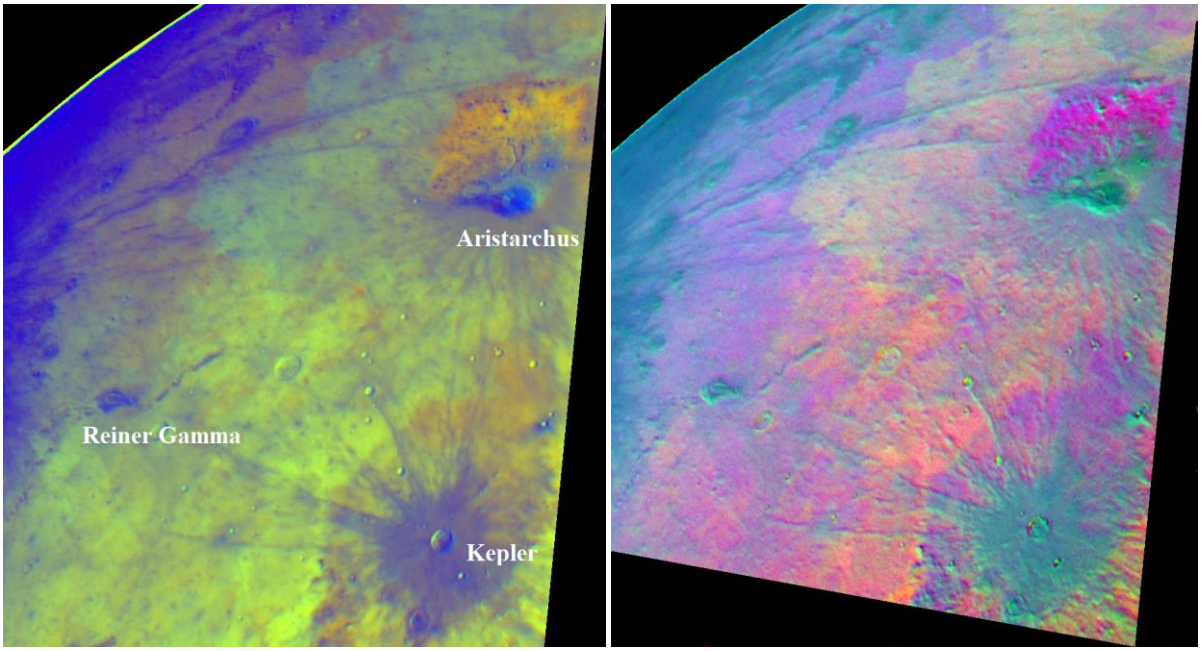

Figure 2: Color composites of telescopic spectropolarimetric image dataset 2 of western Oceanus Procellarum. Left: Logarithmic intensity ratio composite (R channel: R/U, G channel: R/I, B channel: U/R). Right: Color composite of the scores of the first three principal components of the fraction *P* of linear polarization in the UBGRI bands.

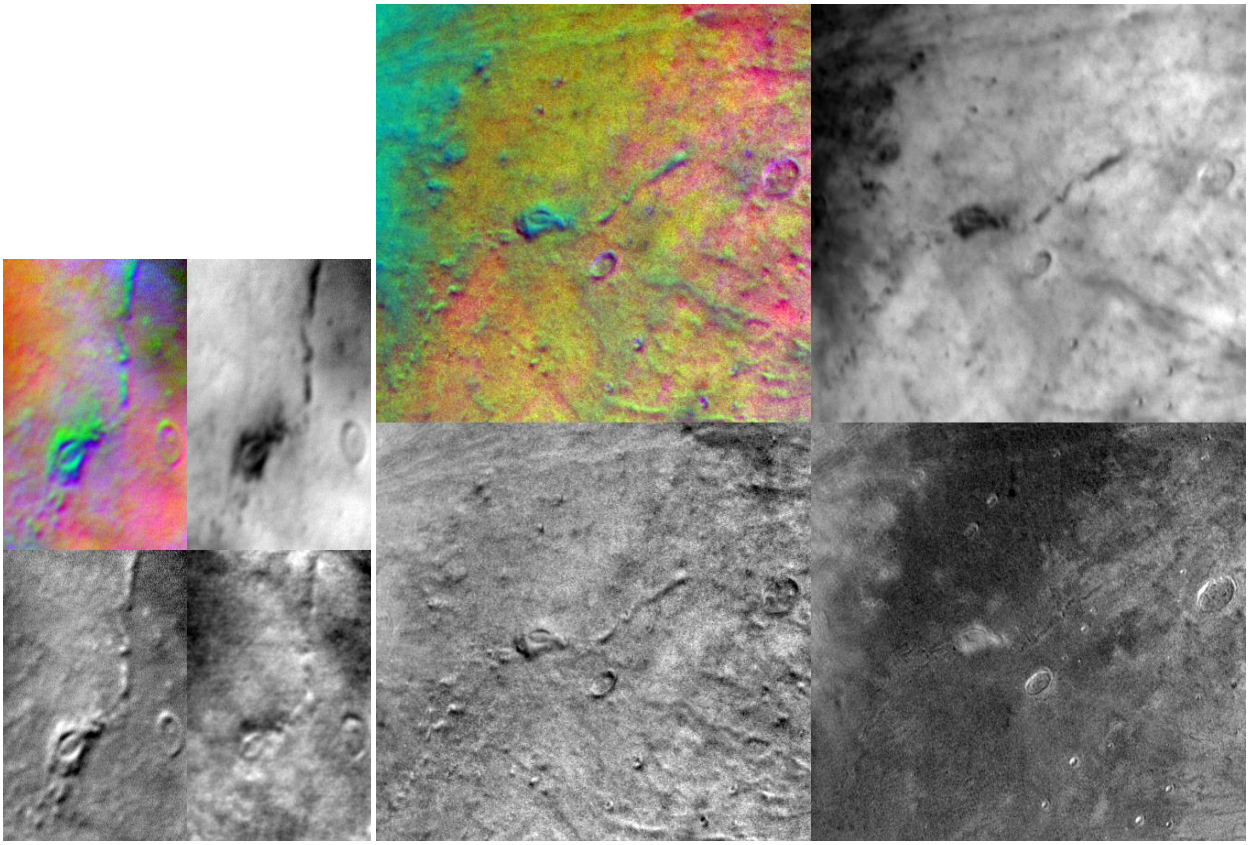

Figure 3: Reiner Gamma area: Scores of the first three principal components of the linear polarization fraction in the different spectral bands, displayed as color composites and grayscale maps (first row: PC1, second row: PC2 and PC3). Left: Dataset 1. Right: Dataset 2. Only data from the areas shown were used for computing the corresponding PCAs.